ARID ZONE JOURNAL OF ENGINEERING, TECHNOLOGY & ENVIRONMENT
AZOJETE June 2026. Vol.22(2):480-491
Published by the Faculty of Engineering, University of Maiduguri, Maiduguri, Nigeria.
Print ISSN: 1596-2490, Electronic ISSN: 2545-5818
https://doi.org/10.63958/AZOJETE/2026/22/02/025
www.azojete.com.ng

ORIGINAL RESEARCH ARTICLE

INVESTIGATING THE COMBINED EFFECT OF RECONDUCTORING AND DG PLACEMENT ON THE LOAD HOSTING CAPACITY OF RADIAL DISTRIBUTION NETWORKS

O. N. Omogbai

Department of Electrical/Electronic and Computer Engineering, Afe Babalola University Ado-Ekiti, Nigeria
Corresponding author's email: omogbaino@abuad.edu.ng

ARTICLE INFORMATION

Received: 2nd April 2026
Revised: 2nd May 2026
Accepted: 8th May 2026

Keywords:
Load hosting capacity
Reconductoring
DG placement
Radial distribution networks
Impedance characteristics

ABSTRACT

The increasing penetration of distributed generation (DG) and the need to accommodate load growth have made load hosting capacity (LHC) a key issue in radial distribution network planning; and feeder reconductoring remains a viable means of modifying network impedance and efficiency. However, the combined influence of reconductoring and DG placement on LHC is not fully explored, particularly under constraints such as voltage rise, reverse power flow, and thermal limits. This study was conducted using the IEEE 33-bus radial feeder, where a 2.5 MW DG operating at unity power factor was sequentially placed across all eligible buses under five distinct reconductoring instances. LHC was determined by incrementally increasing system load using quasi-static backward–forward sweep power flow analysis until constraint are violated, Statistical validation using the Kruskal–Wallis H test was used to assess the significance of the observed changes. The results showed that LHC was governed by a nontrivial interaction between conductor impedance and DG location. For instance, low, uniform impedance profiles deferred upstream constraint violations by maximizing LHC (up to 8.65 MW) when the DG was placed at the terminal bus. Further, high trunk impedance reduced LHC and shifted optimal DG placement toward intermediate or near-source buses to prevent voltage dip in weaker branches. Additionally, when strategically installed feeder-wide, highly resistive conductors with improved X/R ratios partially restored terminal DG placement optimality with moderate LHC. The statistical results ($H = 73.03$, $p = 5.20 \times 10^{-15}$) confirmed that these variations are significant and nonrandom, highlighting the importance of coordinated co-optimization of reconductoring and DG placement for maximizing LHC and enabling proactive feeder planning.

1.0 Introduction

The concept of hosting capacity (HC) was necessitated by the need to quantify how a distribution system reacts to additional connections without a breach on the operational standards. The general definition of HC is "the ability for the network to accommodate a specific or combined installed capacity of one or multiple DER technology considering technical, operational, economical, physical, regulatory, equitable and dynamic considerations on a specific circuit without negatively affecting reliability or requiring infrastructure upgrades." (Hashmi, 2025). This definition, while originally DG-tailored, has since extended naturally to load hosting; that is, the maximum load the network can accommodate under any DG penetration level, existing or projected. In other words, one of the most important, yet underexplored, planning metrics is not simply how much DG a network can accommodate, but rather how much additional load the network can serve—a concept increasingly defined as load hosting capacity (LHC).

LHC is usually considered under the voltage, thermal, and protection constraints that are active in a network already penetrated by DG. Reconductoring (replacing existing conductors with higher-ampacity equivalents) and optimal DG placement are some of the technical interventions that modify these constraints, and therefore affect the LHC (Qamar *et al*, 2023; Adegoke, 2024).

Modern distribution systems do face challenges in hosting increasing loads of unprecedented types; while simultaneously coping with the penetration of huge volumes of renewable energy sources (Cavus, 2025). This has heightened the focus on distribution network capacity optimization strategies that can cost-effectively enhance load hosting capacity with minimal reactionary infrastructure replacement.

In long redial rural networks, voltage level constraint is the major concern, while in urban regions, it becomes the ampacity constraint of equipment due to large loads. This spatial dependency of LHC has made it necessary for it to be evaluated bus-by-bus rather than on a network-wide scale (Fatima *et al*, 2024). Ironically, the same DG that strains the system at high generation levels also relieves it at lower levels, creating a non-linear relationship between DG penetration and LHC. Diverse factors affect the LHC such as the resilience of the network to power fluctuations, load type, number of phases, network topology, and constraints as defined in the decision-making framework (Dong *et al*, 2025).

A radial system has one simultaneous path of power delivery to the load. This topology while simple and cost-effective to set up and operate, hinders the network's capacity to redistribute load, and is the main reason that end-of-feeder voltage drops and conductor thermal limits define the LHC ceiling (Lotfi *et al*, 2024).

The primary mechanism by which DG boosts LHC is via current reduction in upstream feeder segments. The energy supplied by the DG is directly utilized by the loads connected to them, so that the flow of power from the main grid to the load is reduced, and power losses as well as the risk of grid overloading is minimized. This upstream relief directly creates thermal headroom for new load connections at downstream or lateral buses (Rudresha *et al*, 2020; Pan *et al*, 2023). Voltage support is complementary to this i.e.; there will be no violation of voltage constraints if the DG is located close to the loads in a distribution feeder and the DG's power factor is in sync with that of the load. The main grid then supplies less power with reduced feeder current and the voltage dip is reduced. This relief in voltage drop along the feeder tends to accommodate additional loads at buses that previously had insufficient voltage margin (Owosuhi, *et al*, 2024).

The study by Okafor *et al*, (2025) on the hosting capacity of distributed energy resources (DERs) and additional loads that can be connected without the breach of operational limits or without the need for network upgrades; found out that when battery energy storage delivers active power, the additional load capacity increases markedly, with more than 50% extra room at the majority of buses. Other studies also reveal that poor siting of DG does not only fail to improve LHC but may actively reduce it by increasing reverse-power-flow currents or creating localized voltage violations (Jain & Gupta, 2024; Saxena *et al*, 2024).

In a recent study, the optimal siting of different types of DG units were used to handle annual growth in system load while satisfying system operational limits; and results using the standard IEEE 33-bus system revealed enhancement in voltage profile, significant reduction in real and reactive power losses, and improvement in load-carrying capacity of distribution feeder sections (Tuka & Ali, 2026). Another study applying genetic algorithms to the IEEE 33-bus network and a real 11 kV feeder, demonstrated that strategic placement of capacitors and solar PV DG along the distribution feeder achieved significant power loss saving with marginal improvement in voltage profiles, thus creating additional capacity for further load connection (Sharma *et al*, 2026). Other studies involving renewable DGs with load variability further show that by modelling DG output stochastically, using Weibull and Beta distributions for solar irradiance and wind speed; the load hosting improvement becomes sensitive to the mismatch between generation and demand, thus, complicating the conventional deterministic assessment (Elseify *et al*., 2024).

The simultaneous application of network reconductoring and DG placement stands as one of the most effective strategies for maximizing LHC in modern distribution networks (Gallego Pareja *et al*., 2023). In several countries, utilities have already adopted reconductoring as a planning tool. Reconductoring projects typically cost less than 50% of the price of new line installations. The economic benefit for reconductoring as a means of increasing LHC therefore parallels that for DG integration, as both objectives allow for increased thermal headroom and improved voltage regulation (Chojkiewicz *et al*, 2024). Further research by Gallego Pareja *et al*., (2023) emphasizes that approaching reconductoring and DG placement as a joint optimization problem yields superior results compared to a sequential approach. Also, the replacing of undersized conductors that

Corresponding author's email address: omogbaino@abuad.edu.ng

have become laden with reverse power currents from solar PV ensured that the network can make room for both the existing DG and additional load without violating thermal constraints (Zenhom *et al*, 2024).

So far, some areas of research interest do exist. First, the bulk of reviewed studies assess DG hosting rather than LHC specifically. Second, the synergistic effect of reconductoring decisions together with DG placement for the specific objective of maximizing LHC in a radial distribution topology has not been frontally addressed. Therefore, considerable knowledge gaps still do exist regarding their combined influence, as their interactive impacts on network impedance, power flow patterns, and constraint violations remain insufficiently studied. The state-of-the-art in distribution network optimization advocates that effective planning requires a holistic approach that synergistically considers multiple enhancement strategies (Masic *et al*, 2025).

This study therefore investigated the synergistic influence of feeder reconductoring and DG placement, on radial distribution network Load Hosting Capacity (LHC). The thrust was to identify the resulting interaction-driven capacity gains, highlight the necessity of co-optimization in decision-making processes as well as enable accurate evaluation and justification of coordinated planning strategies to boost LHC. Network planners could by the results of this research become better informed about these significant influencers of the distribution system dynamics; for an integrated capacity enhancement decision-making.

2. Materials and Method

This study employed a simulation-based framework to study the impact of reconductoring on the Load Hosting Capacity (LHC) of a radial distribution network in the presence of a single 2.5 MW DG unit proactively installed ab initio to accommodate anticipated load growth. On the IEEE 33-bus radial test system (12.66 kV), deterministic, quasi-static power flow analyses were conducted using the backward-forward sweep algorithm deployed in Python. The DG unit was modeled as a PQ bus operating at unity power factor, and was systematically swept through all eligible 32 feeder buses. For each DG location, the load was incrementally distributed in a substation-and-DG-aware manner, until predefined technical constraints were violated. With this iterative procedure conducted on both a premium feeder and various strategically degraded reconductoring cases, with no voltage regulation devices, the study is able to isolate and relatively quantify the violation patterns, capacity enhancements, voltage profile improvements, and line loading variations across all reconductoring cases; relative to DG location. The study however focused on voltage and thermal constraints as they are widely accepted as the predominant operational limits in LHC studies of radial distribution systems with DG (Ismael *et al*, 2019 & Masic *et al*, 2025). The details are in the following sections and Figure 1 summarizes the methods employed in the study.

2.1 Reconductoring Scenarios

Each reconductoring case employs three conductor types as in Table 1 and was modeled by sequentially substituting existing line conductors to modify the branch resistance (R), reactance (X), and ampacity, while preserving the original network topology and the transition locations for the conductor types. The specific conductor impedance parameters for the evaluated reconductoring cases (A through E), are summarized in Table 1. Figure 2 (Baran & Wu, 2002) illustrates the feeder topology and bus indexing used.

Table 1: Impedance of the line types for the reconductoring cases (A - E)

Line Type	Line IDs	R_A, X_A (Ω)	R_B, X_B (Ω)	R_C, X_C (Ω)	R_D, X_D (Ω)	R_E, X_E (Ω)
1	12-17, 20-21, 23-24, 29-32	0.888, 0.486	1.036, 0.74	1.184, 0.846	1.332, 0.952	1.48, 0.635
2	6-11, 18-19, 22, 25-28	0.704, 0.478	0.821, 0.728	0.938, 0.832	1.055, 0.936	1.173, 0.624
3	1 - 5	0.558, 0.47	0.651, 0.716	0.744, 0.818	0.837, 0.92	0.93, 0.614

2.2 Problem Formulation

The problem was formulated as a constrained multi-objective optimization problem that maximizes load growth within acceptable voltage and thermal limits.

Corresponding author's email address: omogbaino@abuad.edu.ng

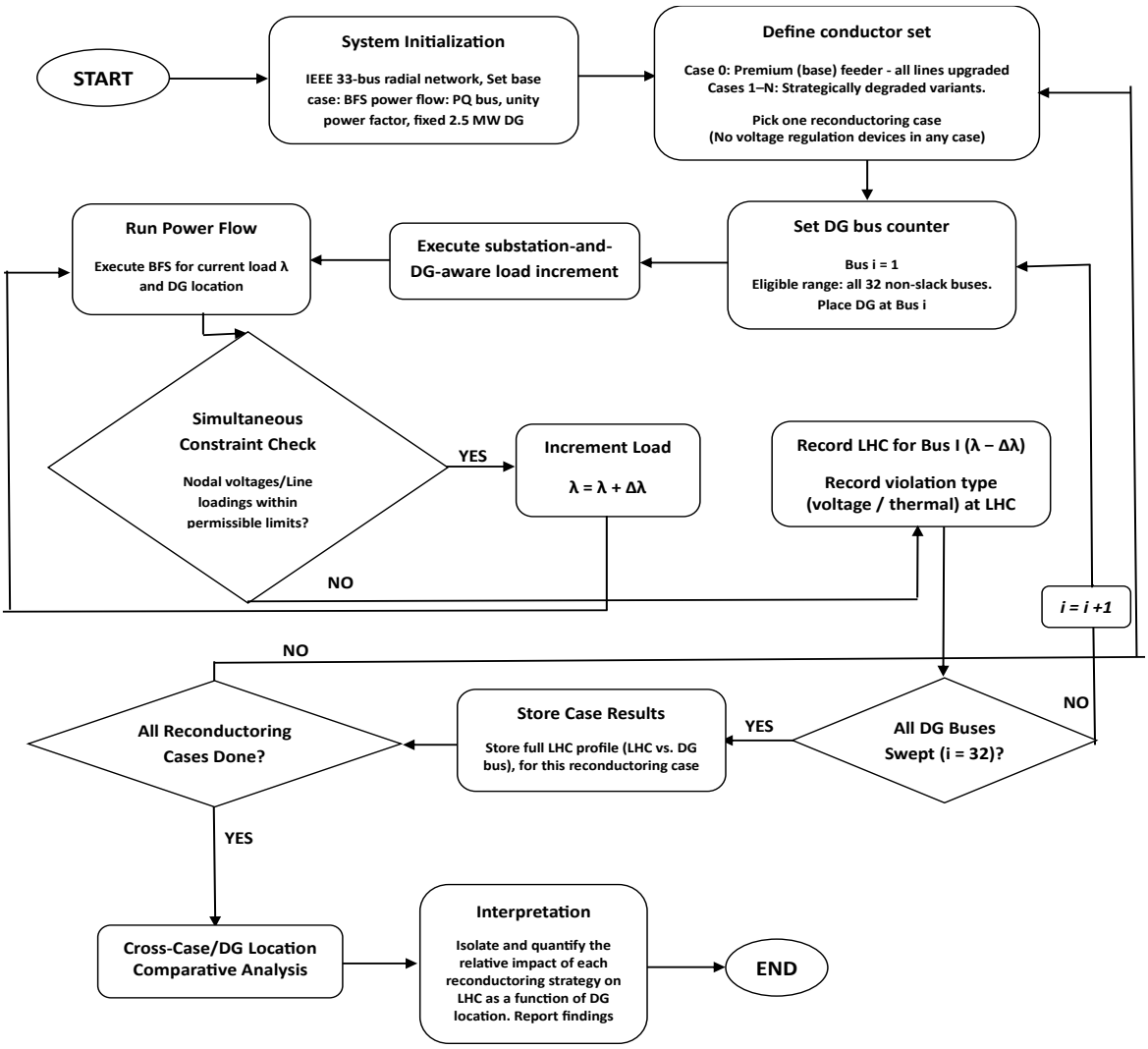

Figure 1: Methods flowchart

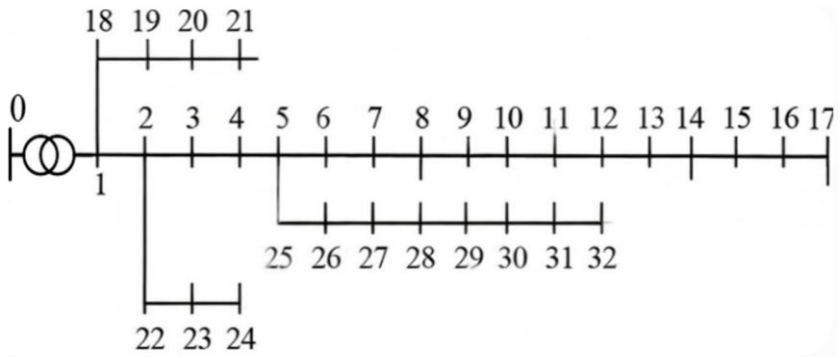

Figure 2: The IEEE 33-bus test feeder with 0 – 32 bus indexing (Baran & Wu, 2002)

2.2.1 *Load hosting strategy*

The strategy uses an aggressive approach that allocates new loads to select buses, by prioritizing closeness to voltage support (substation and DG). A robust iterative normalization process was employed to guarantee precise load allocation that fulfills the following: sums up to the target increment, enforces an upper limit per-bus to prevent unrealistic concentration, and applies a minimum threshold to forestall negligible allocations. Four competing objectives were being optimized i.e., voltage margin, thermal loading, weighted electrical distance, and bus utilization; using the Non-dominated Sorting Genetic Algorithm II (NSGA-II) to prioritize the identification of technical limits for determining the maximum additional load that the feeder can host prior to voltage or thermal constraint violations.

Corresponding author's email address: omogbaino@abuad.edu.ng

2.2.2 *Decision variables*

Each load increment was distributed across *n* candidate buses using weighting vectors ω_i; such that the weights satisfy Equations (1) – (3):

$$\sum_{i=1}^{n} \omega_i = 1, \quad 0 \leq \omega_i \leq 0.6 \qquad 1$$

$$\omega_i = [\omega_1, \omega_2, \ldots, \omega_n] \qquad 2$$

So that the actual incremental load at bus *i,* i.e., $\Delta P_i = \omega_i . P_{inc}$ 3

where ω_i is the fraction of total additional load allocated to bus *I*, P_{inc} is the total system load increment (kW). The ω_i upper bound of 0.6 arose from a preliminary sensitivity analysis; and serves to preclude excessive load being concentrated unrealistically at any given bus, which could otherwise overburden the critical local equipment.

2.2.3 *Objective functions*

Multi-objective hosting capacity formulations as outlined hereafter are well-established in the literature (Al-Majali & Zobaa, 2025; Almutairi *et al,* 2024; Owosuhi *et al*, 2024).

(a) Voltage Regulation

Equation (4) enforces the non-violation of the specified voltage limits, while Equations (5) – (6) penalizes all unacceptable voltage deviations.

$$min\ f_1(w) = -V_{margin} + 0.3\sigma V + 0.2\Delta V + P_V + P_{OV} \qquad 4$$

where, $V_{margin} = min_i(V_i - V_{min})$ is the safety margin for voltage dip; which is meant to stay non-negative.

V_i, V_{min} = per unit voltage magnitude at bus *i* and the worse-case minimum voltage (0.9 pu) respectively.

σV = standard deviation of bus voltages accounting for minimal spatial variation of the system voltage profile. This term is weighted below the V_{margin} to give more emphasis to the latter.

ΔV = voltage range to limit localized constraint violations

Penalty terms for undervoltage, P_V = 20.max (0, 0.92 - V_{min}) 5

Penalty terms for overvoltage, P_{OV} = 10.max (0, V_{max} – 1.03) 6

A more weighted P_V is intended for its greater operational significance in load growth scenarios.

(b) Thermal Loading Regulation

To ensure ample thermal headroom for load fluctuation, uncertainty and contingency operation, a target soft limit of 70% loading (preserving optimization flexibility) was selected and appropriately penalized using Equations (7) and (8) respectively i.e.,

$$min\ f_2(w) = |L_{max} - 70\%| + P_L \qquad 7$$

Soft penalty term: P_L = 0.5.max (0, L_{max} – 85%) 8

where, $L_{max} = max_j(L_j)$; maximum line loading, L_j = the percentage loading of line *j*

With 0.5 (0.3 - 0.7 actually produced comparable results) as the penalty scaling factor, thermal constraints are prevented from dominating over voltage-related objectives, thereby guiding the solution search.

Corresponding author's email address: omogbaino@abuad.edu.ng

(c) Proximity to Substation or DG

In line with Equation (9), the strategy for the distribution of additional loads considers proximity to the sources of voltage support i.e.,

$$min\ f_3(w) = \frac{\sum_{i=1}^{n} \omega_i P_i d_i}{\sum_{i=1}^{n} \omega_i P_i} \quad 9$$

where, P_i = the base active load at bus *I*, d_i = the electrical distance (line impedance magnitudes) between bus *i* and the closest voltage support node (substation or DG).

(d) Load Spatial Spread by Constrained Normalization

After normalizing the decision variables, an iterative constraint-enforcement and load redistribution was performed over 10 cycles., with a final renormalization step to ensure that the allocation weights add up to unity under a 10^{-6} tolerance. A minimum threshold of 1 kW ensured that only realistic load connections were considered as enforced by Equations (10) and (11) i.e.,

$$min\ f_4(w) = \frac{Set\ of\ Insignificant\ Buses}{Total\ number\ of\ candidate\ bus} = \frac{|\{i: \omega_i < \alpha_{min}\}|}{n} \quad 10$$

where, the minimum significant allocation ratio $\alpha_{min} = \frac{P_{min}}{P_{inc}}$ 11

P_{min} = realistic minimum load magnitude (kW)

2.2.4 *Constraints*

Equations (12) and (13) represents the necessary constraints for the determination of the load hosting limits under the various scenarios.

Voltage constraints: $0.9 \leq V_i \leq 1.05$ pu $\quad \forall_i \in \{0, \ldots, 32\}$ 12

Thermal constraints: $L_j \leq 100\%, \quad \forall_j \in \{1, \ldots, 32\}$ 13

The lower voltage limit typically captures worst-case conditions during load growth; whereas the upper bound mainly constrains DG-induced voltage rise. Emergency loading scenarios (typically 120 - 130%) were omitted, since steady state planning conditions are assumed rather than short-term contingency.

2.2.5 *Incremental loading strategy*

For the purpose of this study, the load hosting capacity (LHC) is defined as the total kW of load the feeder can accommodate before the violation of voltage or thermal constraint. To select the next increment size, a weighted combination ϕ of voltage and line loading margins was dynamically computed, as in Equation (14), to track the point at which the iterative load increase first violates the constraints. Assuming voltage margin as the more dominant limiting factor, then:

$$\phi = 0.65\frac{V_i - V_{min}}{1.0 - V_{min}} + 0.35\frac{L_{max} - L_j}{L_{max}} \quad 14$$

A linear combination arose from the observed poor correlation between voltage and thermal margins during preliminary tests. For fewer iterations of load increment with precision, the process begins with an increment of 500 kW. At $\phi > 30\%$, the strategy expands to 1000 kW increments, then it refines the search with 500 kW increments again at $15 < \phi \leq 30\%$. At the precision phase ($\phi \leq 15\%$), 250 kW or less then becomes the load increments, until the process finally terminates at the first violation of voltage or thermal constraints.

2.3 Solution Algorithm

The NSGA-II was selected for its well-known robustness in handling nonlinear, multi-objective power system problems. With a flat-start method of initialization, key parameters include; population size (80), maximum

Corresponding author's email address: omogbaino@abuad.edu.ng

generations (120), convergence tolerance (10^{-4}), simulated binary crossover probability (0.95), distribution index (10), polynomial mutation distribution index (15), and BFS mismatch tolerance (10^{-5} MVA).

3. Results and Discussion

3.1 Preliminary Statistical Significance Test

Given the non-Gaussian distribution and unequal variance of the obtained LHC values, a distribution-free hypothesis test i.e., the Kruskal–Wallis H test, was selected as an appropriate nonparametric method for the comparison of the five sets of the LHC results. The test yielded a large test statistic (H = 73.03) with a corresponding p-value of 5.20×10^{-15}. This result confirmed that the observed LHC differences among reconductoring cases were statistically significant, systematic and not a spurious outcome of random variability.

3.2 Load Hosting Capacity Under a Feeder-Wide Single-DG Sweep

Figure 3 shows the LHC obtained from a feeder-wide sweep of a single 2500 kW DG across the IEEE-33 bus system under five reconductoring scenarios (Cases A - E).

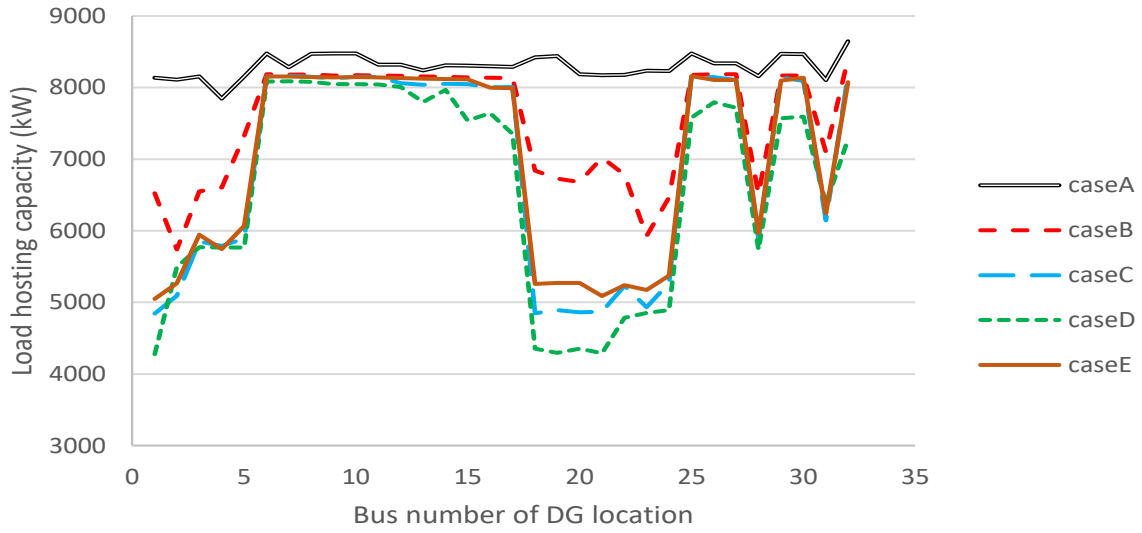

Figure 3: LHC for different DG placements under different reconductoring cases

The reconductoring scenarios introduced a progressive change in branch impedance in the following order: $R_A < R_B < R_C < R_D < R_E$and $X_A < X_B < X_C < X_D$. However, Case E exhibited a reduced reactance relative to Case D despite a higher resistance, resulting in an elevated R/X ratio. Figure 3 showed distinct spatial regimes along the feeder. For DG placements close to the substation (Buses 1- 5), higher impedance cases exhibited suppressed LHC near the source with rapid recovery by Bus 6, since the DG location offered limited downstream voltage support while driving elevated currents through lengthy and high-impedance paths. For DG located at the mid-feeder region (Buses 6 - 17), all scenarios converged to a narrow LHC band of approximately 8 MW, indicating effective feeder partitioning by the DG and reduced cumulative voltage drops on both partitions, which appeared to almost cancel out the influence of reconductoring.

A significant lateral branching emerged for Buses 18 - 24, where LHC began to diverge across cases. DG placement at these buses increasingly interacted with asymmetric downstream impedances, rendering Cases B - E sensitive to both the R/X ratio and the branching topology, while Case A remained virtually constant owing to its higher electrical stiffness. For DG at deep-feeder region (Buses 25–32), pronounced oscillatory LHC behavior dominated, particularly for Cases B – E; peaking at branching nodes that supply multiple downstream paths and dipping at series buses where upstream impedance aggregated without parallel relief.

In sum, Case A yielded a spatially uniform LHC profile owing to low impedance and minimal voltage deviation. Cases B and C introduced moderate spatial variability with constraint violation that occurred relatively early for DG at remote buses, while Case D defined the performance floor, where elevated R and X brought about

Corresponding author's email address: omogbaino@abuad.edu.ng

premature violations. In contrast, Case E illustrated that reduced *X* tended to check reactive-power-driven voltage dip, bringing about superior LHC performance relative to Case D despite its higher *R*.

3.3 Strategic Migration of Optimal DG Placement

From Table 2, it can be observed that the migration of optimal (maximum LHC) DG location upstream was primarily as a result of impedance stress caused by reconductoring, and it was context-dependent i.e., it was generally upstream bound under high *X* and *R*, and downstream-bound in *R* dominant feeders; so as to leverage voltage support and maximize hosting capacity.

Table 2: Optimal DG buses with the corresponding LHC

Case	Conductor Impedance	Optimal DG Bus	LHC (kW)
A & B	Low, Uniform	32 (Terminal)	8646 & 8400
C	Moderately High	25 (Intermediate Lateral)	8158
D	Highest, non-uniform	7 (Near Source)	8087
E	High R, Lower X	32 (Terminal)	8178

Therefore, reconductoring was observed to influence a systematic migration in optimal DG placement, governed by electrical distance and the resulting feeder bottlenecks. However, beyond a 40 - 50% increase in resistance (e.g., Case C), the effectiveness of distal DG placement began to wane; highlighting the importance of targeted conductor upgrades along the main feeder trunk (Buses 0 - 5) to preserve optimal distal DG placement and relieve upstream bottlenecks.

3.4 Feeder-Wide Line Loading and Voltage Profile at Maximum Load Hosting

For the purpose of analysis, feeder-wide voltage and line loading profiles corresponding to the optimal scenarios (DG placement that maximizes load hosting capacity) were considered. The analyses in this section are all with reference to Table 2 and Figures 4 and 5.

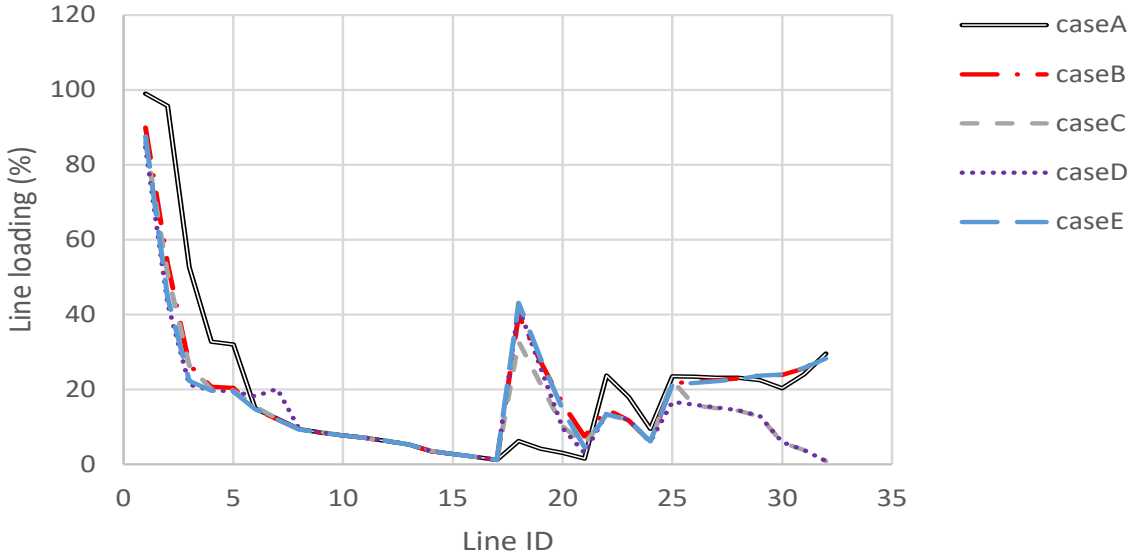

Figure 4: Line loading profile comparison at maximum load hosting.

In Case A, the low impedance network backbone was observed to favor the optimal DG placement at Bus 32, and this facilitated efficient reverse power flow and a clear end fed voltage support. In agreement with the line loading, the voltage dipped steadily from the substation (Bus 0) to about 0.908 pu near Bus 17, consistent with normal forward supply, then recovered along the laterals. Branch 1(Lines 18 - 21) remained close to nominal voltage with the minimum line loading, indicating minimal reverse flow. Branch 2 (Lines 22 - 24) showed moderate and largely stable voltages that suggested steady loading. A monotonic voltage rise toward Bus 32 is observed in Branch 3 **(**Lines 25 - 32**)**, confirming strong distal DG injection that makes up for downstream drops and exported excess power upstream. This reverse flow through a low-impedance path, strongly drove the feeder head close to its thermal limit but largely spared the laterals. Constraints were therefore shifted

Corresponding author's email address: omogbaino@abuad.edu.ng

upstream. Consequently, efficient bidirectional power flow that minimizes reverse power losses became the case. These ultimately culminated in the highest load hosting capacity of 8,646 kW among all cases under study.

In Case B, the higher network backbone impedance was observed to favor the optimal DG placement still at Bus 32 stifles upstream reverse power flow, thereby unloading the feeder head and rerouting stress toward proximal laterals. Voltage tended to drop more steeply close to the substation but reached a similar minimum around Bus 17, indicating reduced through currents. Compared to case A, Branch 1 now showed significant voltage dip due to strong local reverse flow (sharp spike in line loading as seen in Figure 4) against higher impedance, whereas the short and peripheral Branch 2 (low local current swings relative to its impedance) remain largely the same. Branch 3 maintained a considerable end fed voltage rise, with a higher terminal voltage than in Case A as impeded upstream export encourages greater local buildup of reverse power. Overall, the backbone impedance acted as a flow valve that transferred thermal and voltage stress from the feeder head to adjacent laterals; slightly decreasing the bidirectional power flow efficiency and consequently reducing the load hosting capacity to about 8,400 kW.

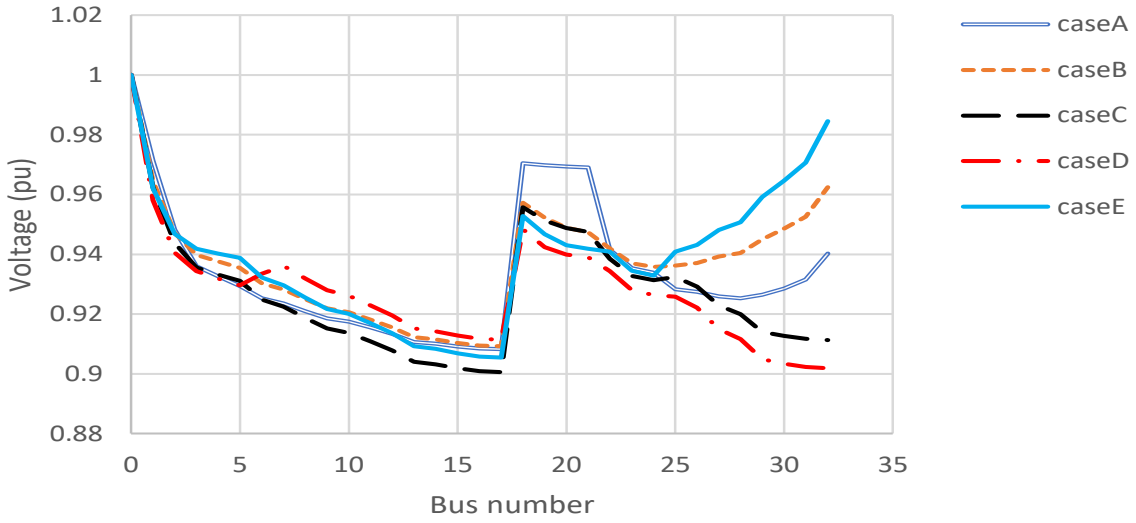

Figure 5: Voltage profile comparison at maximum load hosting.

In Case C, the even higher network backbone impedance was observed to favor the optimal DG relocation to Bus 25, and this decoupled upstream and downstream dynamics; fundamentally rerouting power flow. Voltage dipped more steeply along the main feeder, reaching the lowest minimum near Bus 17, indicating increased joule losses despite the slight drop in reverse currents. Branch 1 still experienced voltage depression (similar to case B) from upstream-bound flow, but its magnitude has dropped because the DG was no longer distal and the export path is now shorter. Branch 2 remained largely unchanged. Branch 3 now drastically shifted to a steady voltage decline toward the terminus, indicating that the mid-feeder DG took care of local demand and collapsed through-current beyond Bus 25. This localization of supply tended to relieve upstream thermal stress but shrank the downstream voltage margins, thereby reducing overall utilization and reducing the load hosting capacity to 8,158 kW.

In Case D, the even much higher network impedance backbone was observed to favor a deeper optimal relocation of the DG upstream to Bus 7, and this strongly limited long-distance bidirectional flow and confined the power effects around the injection point. Voltages clearly spiked near the DG but dropped sharply downstream, with Branch 1 experiencing the lowest voltage sag and heavy proximal loading due to intense reverse flow. Branch 2 remained stable. Branch 3 showed a drastic downstream unloading and the lowest terminal voltages, indicating near-collapse of through-current beyond the mid-feeder. Impedance transitions near the DG created the observed localized current loops/spikes, thereby crowding the thermal stress around the mid-feeder. These increased losses, voltage gradients, and distal undervoltage all limited overall utilization, resulting in the lowest load hosting capacity of 8,087 kW.

In Case E, under high-impedance and reduced X/R ratio, the network appeared to re-find optimal placement of the DG distally at Bus 32. The backbone experienced a steep voltage profile that dipped to around 0.905 pu, while Branch 1 experienced severe upstream reverse-flow loading similar to Case D; thereby driving high proximal currents and joule losses. Branch 2 remained largely unchanged, and Branch 3 exhibited the sharpest

Corresponding author's email address: omogbaino@abuad.edu.ng

monotonic voltage rise toward Bus 32, peaking at 0.985 pu; indicating strong end-fed DG support and the buildup of reverse currents. The lower X/R ratio amplified the impact of active-power injection, thus, boosting distal voltage without considerable mid-feeder spikes. Overall, thermal constraints stayed concentrated at the feeder head, and the LHC recovers modestly to 8,178 kW.

Overall, DG location governed the branch loading patterns, while impedance and the X/R ratio primarily modulated the voltage profiles as well as the routing of power flow - highlighting the need for strategic co-optimization of DG siting and feeder impedance to maximize the LHC. The findings are strongly supported in closely related studies (Alyu *et al*, 2023; Barker & De Mello, 2000; Takele, 2022)

3.5 Constraint Violation Analysis

Table 3: Network constraint violation pattern (T = Thermal and V = Voltage)

Violation Pattern (Case A-B-C-D-E)	DG Bus Count	DG Bus Location
T - V - V - V – V	13	1, 2, 3, 5, 18, 19, 20, 21, 22, 23, 24, 28, 31
T - T - T - V – T	10	13, 15, 16, 17, 25, 26, 27, 29, 30, 32
T - T - T - T – T	8	6, 7, 8, 9, 10, 11, 12, 14
V - V - V - V – V	1	4

From Table 3, it was observed that for the feeder topology under study, the thermal-voltage constraints transition is a function of both line impedance and the location of the DG/substation. Increasing total impedance via reconductoring generally heightens voltage-rise sensitivity, causing a systemic shift where voltage limits bind more stringently and before thermal limits. At remote and lateral buses, low-impedance scenarios (A–C) tended to be constrained by thermal overloads, whereas higher impedance as in Case D shifted the bottleneck to voltage. However, elevated R/X ratio as in Case E, intensified resistive voltage rise, which can alter the system's sensitivity profile and return the prevailing constraint at certain buses to thermal.

In contrast, DG placement on the electrically strong main feeder, specifically buses 6 - 12 and 14, results in thermal limits becoming the overriding constraint across all cases. Their proximity to the substation keeps sensitivity to voltage-rise low enough that ampacity limits were reached before voltage thresholds were breached, even with higher R/X ratios as in Case E.

Unlike adjacent buses (thermal-limited) or more distant ones (weaker voltage effect, Bus 4 represents a unique intermediate bottleneck, as injected power here, triggered a sharp spike in upstream voltage without heavily loading downstream lines; regardless of reconductoring. So, the feeder with DG at Bus 4 remained invariably voltage binding. Ultimately, while reconductoring at strong locations majorly influences thermal hosting capacity, DG placement at sensitive or proximal locations ensured that voltage remained the binding constraint. Overall, effective feeder planning to defer voltage violations and unlock usable DG or load capacity requires a comprehensive spatial analysis of hosting capacity, strategic voltage control as well as targeted reconductoring of electrically weak sections.

4. Conclusion

This study focused on the impact of reconductoring and distributed generation (DG) placement on the load hosting capacity (LHC) of a radial distribution system typified by the IEEE 33-bus system with a 2.5 MW unity power factor DG. From the obtained results, the sequential DG placement under different reconductoring cases revealed that low and uniformly distributed impedance profiles can enhance LHC up to a margin of about 10% (for reconductoring only) and at least 60 % (for DG + reconductoring); achieved when DG is installed at terminal buses. Conversely, high trunk impedance reduced LHC and shifted optimal DG placement toward intermediate or upstream buses due to the violation of voltage limits in weaker branches. It was also observed that when strategically placed feeder-wide, conductors with improved X/R ratios partially reestablished an optimal terminal DG placement, yielding moderate improvements in LHC.

Statistical analysis using the Kruskal–Wallis H test confirmed that the observed variations in LHC are significant and non-random ($H = 73.03$, $p = 5.20 \times 10^{-15}$), underscoring the strong dependency of network performance on coordinated design decisions. Overall, the results from the study contributed by highlighting that optimal enhancement of load hosting capacity requires a joint consideration of reconductoring strategy and DG siting,

Corresponding author's email address: omogbaino@abuad.edu.ng

rather than treating them as isolated planning variables, thereby supporting more proactive and integrated distribution feeder planning.

Future work should extend the analysis to varying types/number of DG units with coordinated placement and sizing for better practical relevance. Time-series and probabilistic modeling will further capture renewable intermittency, load variability, and forecast uncertainty in LHC estimation. Also, hybrid metaheuristics or AI-based methods, can be developed for simultaneous reconductoring and DG allocation, under multi-objective criteria. Further investigation is needed to investigate the effect of increased DG penetration and reconductoring on fault levels and relay performance. Real distribution network data with energy storage systems and regulatory constraints, particularly in emerging grid environments will further improve the practical relevance and applicability of the findings.

Acknowledgment

The author sincerely acknowledges the research support of the management Afe Babalola University Ado Ekiti during the course of this study; as well as the constructive feedback from reviewers and colleagues that helped improve this work.

References

Adegoke, SA., Sun, Y., Adegoke, AS. and Ojeniyi, D., 2024. Optimal placement of distributed generation to minimize power loss and improve voltage stability. *Heliyon*, *10*(21).

Al-Majali, B. and Zobaa, AF., 2025. Analyzing bi-objective optimization Pareto fronts using square shape slope index and NSGA-II: A multi-criteria decision-making approach. Expert Systems with Applications, 272:126765. https://doi.org/10.1016/j.eswa.2025.126765

Almutairi, SZ., Alharbi, AM., Ali, ZM., Refaat, MM. and Aleem, SHA., 2024. A hierarchical optimization approach to maximize hosting capacity for electric vehicles and renewable energy sources through demand response and transmission expansion planning. Scientific Reports, 14(1): 15765.

Alyu, A.B., Salau, AO., Khan, B., & Eneh, JN. 2023. Hybrid GWO-PSO based optimal placement and sizing of multiple PV-DG units for power loss reduction and voltage profile improvement. Scientific Reports, 13(1): 6903.

Baran, ME. and Wu, FF., 2002. Network reconfiguration in distribution systems for loss reduction and load balancing. IEEE Transactions on Power delivery, 4(2): 1401-1407.

Barker, PP., & De Mello, RW. 2000. Determining the impact of distributed generation on power systems. I. Radial distribution systems. In 2000 Power Engineering Society Summer Meeting (Cat. No. 00CH37134) (Vol. 3, pp. 1645-1656). IEEE.

Cavus, M. 2025. Advancing Power Systems with Renewable Energy and Intelligent Technologies: A Comprehensive Review on Grid Transformation and Integration. Electronics, 14(6): 1159.

Chojkiewicz, E., Paliwal, U., Abhyankar, N., Baker, C., O'Connell, R., Callaway, D. and Phadke, A., 2024. Accelerating transmission capacity expansion by using advanced conductors in existing right-of-way. *Proceedings of the National Academy of Sciences*, *121*(40): 2411207121.

Dong, C., Yu, T., Pan, Z., Wu, Y., Wang, Z., Wang, Y. and Wang, K., 2025. Renewable energy hosting capacity assessment in distribution networks based on multi-strategy improved whale optimization algorithm. *IET Renewable Power Generation*, *19*(1): e12994.

Elseify, MA., Hashim, FA., Hussien, AG., Abdel-Mawgoud, H. and Kamel, S., 2024. Boosting prairie dog optimizer for optimal planning of multiple wind turbine and photovoltaic distributed generators in distribution networks considering different dynamic load models. *Scientific Reports*, *14*(1): 14173.

Corresponding author's email address: omogbaino@abuad.edu.ng

Fatima, S., Püvi, V., Lehtonen, M. and Pourakbari-Kasmaei, M., 2024. A review of electric vehicle hosting capacity quantification and improvement techniques for distribution networks. *IET Generation, Transmission & Distribution*, *18*(6): 1095-1113.

Gallego Pareja, LA., López-Lezama, JM. and Gómez Carmona, O., 2023. Optimal integration of distribution network reconfiguration and conductor selection in power distribution systems via MILP. *Energies*, *16*(19): 6998.

Hashmi, MU., 2025, June. DER hosting capacity for distribution networks: definitions, attributes, use-cases and challenges. In *IET Conference Proceedings CP922* (Vol. 2025, No. 14, pp. 541-546). Stevenage, UK: The Institution of Engineering and Technology.

Ismael, SM., Aleem, SHA., Abdelaziz, AY. and Zobaa, AF., 2019. State-of-the-art of hosting capacity in modern power systems with distributed generation. Renewable energy, 130: 1002-1020

Jain, A. and Gupta, SC., 2024. Optimal placement of distributed generation in power distribution system and evaluating the losses and voltage using machine learning algorithms. Frontiers in Energy Research, 12: 1378242.

Lotfi, H., Hajiabadi, ME. and Parsadust, H., 2024. Power distribution network reconfiguration techniques: A thorough review. *Sustainability*, *16*(23): 10307.

Masic, F., Saric, M., Hivziefendic, J. and Dzemic, Z., 2025. Hosting capacity in smart distribution systems using OpenDSS tool and Monte Carlo-based methodology. Science and Technology for Energy Transition, 80: 2.

Okafor, CE., Olasoji, AO., Mditshwa, M., Folly, KA. and Oyedokun, DT., 2025, September. Analysis of the Hosting Capacity of a Distribution Network Integrated with Solar Photovoltaics Plants, Battery Energy Storage Systems, and Electric Vehicles. In *2025 IEEE PES/IAS PowerAfrica* (pp. 1-6). IEEE.

Owosuhi, A., Hamam, Y. and Munda, J., 2024. A New Framework for Active Loss Reduction and Voltage Profile Enhancement in a Distributed Generation-Dominated Radial Distribution Network. *Applied Sciences*, *14*(3): 1077.

Pan, S., Maleki, S., Lakshminarayana, S. and Konstantinou, C., 2023, October. Optimal placement and power supply of distributed generation to minimize power losses. In *2023 IEEE International Conference on Communications, Control, and Computing Technologies for Smart Grids (SmartGridComm)* (pp. 1-6). IEEE.

Qamar, N., Arshad, A., Mahmoud, K. and Lehtonen, M., 2023. Hosting capacity in distribution grids: A review of definitions, performance indices, determination methodologies, and enhancement techniques. *Energy Science & Engineering*, *11*(4): 1536-1559.

Rudresha, SJ., Ankaliki, SG. and Ananthapadmanabha, T., 2020. Impact of DG integration in distribution system on voltage stability and loss reduction for different loading conditions. *International Journal of Recent Technology and Engineering*, *8*(5): 2177-2181.

Saxena, N., Pandit, M. and Srivastava, L., 2024. Multi-objective DG placement in radial distribution systems using the Ibl logic algorithm. *Frontiers in Energy Research*, *12*: 1453715.

Sharma, A., Chakraborty, P., Datta, M. and Hasan, KN., 2026. Optimal Placement and Sizing of PV-Based DG Units in a Distribution Network Considering Loading Capacity. *arXiv preprint arXiv:2602.16565*.

Takele, H. 2022. Distributed generation adverse impact on the distribution networks protection and its mitigation. Heliyon, 8(6).

Tuka, MB. and Ali, SE., 2026. Optimal allocation and sizing of distributed generation for improvement of distribution feeder loss and voltage profile in the distribution network using genetic algorithm. *Measurement and Control*, *59*(2): 217-231.

Zenhom, ZM., Aleem, SHA., Zobaa, AF. and Boghdady, TA., 2024. A comprehensive review of renewables and electric vehicles hosting capacity in active distribution networks. *IEEE Access*, *12*: 3672-3699.

Corresponding author's email address: omogbaino@abuad.edu.ng